Petrology, geochemistry (Geochronology)

Emplacement of the Lavadores granite (NW Portugal): U/Pb and AMS results

Mise en place du granite de Lavadores (Portugal nord-occidental) : résultats U/Pb et ASM

Helena C.B. Martins *, Helena Sant'Ovaia, Joana Abreu, Miguel Oliveira, Fernando Noronha

Geology Centre/Department of Geosciences, Environment and Spatial Planning, Faculty of Sciences, Porto University, Rua do Campo Alegre 4169-007 Porto, Portugal

ABSTRACT

Studies of Anisotropy of Magnetic Susceptibility (AMS) and U-Pb geochronology, in zircon fractions, were carried out in a magnetite type-granite, the Lavadores granite, which is an example of a late to post-orogenic Variscan granite in northern Portugal (NW Iberian Peninsula). The U-Pb zircon analyses yield an age of 298 ± 11 Ma that is considered to be the emplacement age of this granite and thus suggesting a post-tectonic emplacement. This is also supported by the magmatic nature of the microstructures. Magnetic lineations are subvertical and magnetic foliations display a general WNW-ESE subvertical pattern consistent with a dextral kinematic. These AMS data suggest that the emplacement of the Lavadores granite was controlled by a major mechanical anisotropy formed by transtensional structures associated with the Porto-Tomar shear zone.

© 2011 Académie des sciences. Published by Elsevier Masson SAS. All rights reserved.

RÉSUMÉ

Une étude de l'anisotropie de susceptibilité magnétique (ASM), couplée à la datation U-Pb, sur fractions de zircon, a été menée dans le granite de Lavadores, un granite à magnétite, qui est un bon exemple de granites Varisques, tardi à post-orogénique. Les analyses U-Pb sur zircon ont donné un âge à 298 ± 11 Ma interprété comme l'âge de mise en place post-tectonique du granite de Lavadores. Les microstructures magmatiques confirment cette mise en place post-tectonique. Les linéations magnétiques sont verticales et les foliations magnétiques présentent un fort pendage avec une orientation WNW-ESE en accord avec une cinématique dextre. Ces données ASM suggèrent que la mise en place du granite de Lavadores a été contrôlée par une anisotropie mécanique majeure qui correspond à des structures transtensives associées à la zone de cisaillement de Porto-Tomar.

© 2011 Académie des sciences. Publié par Elsevier Masson SAS. Tous droits réservés.

1. Introduction

It is well documented that the ascent and emplacement of many granites intrusions is significantly controlled by tectonic activity along faults and shear zones, in different tectonics settings (Castro, 1986; Hutton, 1988; Ingram and Hutton, 1994; Speer et al., 1994; Tikoff and Saint Blanquat, 1997). This relationship is well demonstrated by the synchronous timing and spatial association of many Variscan granites in the Variscan belt (Faure, 1995; Faure and Pons, 1991; Faure et al., 2002; Gébelin et al., 2006, 2007, 2009; Joly et al., 2009).

---

* Corresponding author.
  E-mail address: hbrites@fc.up.pt (Helena C.B. Martins).

Outstanding features of the internal zone of the Iberian Variscides, the Central Iberian Zone, are a complex shear zone network and a intensive late to post-orogenic Variscan magmatism with the most active period spanning broadly the time between c. 320 and 290 Ma (Dias et al., 1998, 2009; Fernández-Suárez et al., 2011; Martins et al., 2009). In northern Portugal, this magmatic activity has left large granitoid plutons which presented highly contrasted compositions and whose emplacement was in most cases associated to major Variscan structures, namely shear zones and strike slip faults. The Lavadores granite emplacement was controlled by one of the most important structure crossing the Variscan basement, the Porto-Tomar Shear Zone (PTSZ). The PTSZ is a north-south dextral transform fault that was active throughout much of the Devonian as well as the Variscan (Dias and Ribeiro, 1995; Ribeiro et al., 2009). Other authors propose that the PTSZ is a major fault only structured since the beginning of the Variscan orogeny (Pereira et al., 2010).

The first Rb-Sr geochronological data of the Lavadores granite were obtained by Mendes (1967) in biotite and Silva (1995) in whole rock, which respectively gave an age of 346 ± 14 Ma and 314 ± 11 Ma, suggesting a syntectonic emplacement. However, the well-known limitations of the Rb-Sr isotopic system and because these ages are not in agreement with field and structural data, lead us to the development of a U-Pb zircon geochronology. The aim of this work is to better constrain the emplacement age of the Lavadores granite (northern Portugal) with a multidisciplinary approach: U-Pb geochronology data and structural characterization through a study of Anisotropy of Magnetic Susceptibility (AMS). Studies of AMS were preceded by detailed geological mapping and complemented by petrographic and microstructural observations. The AMS studies were performed in the Lavadores granite as well as in its country rocks.

The main results of this study show that this granite is post-tectonic and ascent and emplaced along a non-active ductile extensional shear zone.

2. Geological setting

The tectonometamorphic and magmatic features of the Western Europe Variscan belt have been explained by the collision of Laurentia-Baltica with Gondwana (Lagarde et al., 1992; Matte, 1991) and has taken place from Early Devonian to Mid-Carboniferous (390–330), followed by post-thickening extension from the Mid-Carboniferous to the Permian times (330–280). The innermost zone of the Iberian Variscan Belt constitutes the Central Iberian Zone (CIZ) in which three main ductile Variscan deformation phases (D_1, D_2 and D_3) were recognized (Noronha et al., 1979; Ribeiro, 1974; Ribeiro et al., 1990). The D_1 and D_2 deformation phases correspond to the collision stage of the Variscan orogeny whereas the last ductile deformation phase D_3, Namurian-Westphalian in age, is related to the post-thickening extension tectonic regime. This event develops open to tight vertical folds with subhorizontal axes and subvertical shear zones with sinistral or dextral wrench movements and was followed by a fragile deformation

phase giving rise to a set of conjugate strike-slip faults (NNW-dextral and NNE-sinistral), pointing to a Late-Variscan main compression around north-south (Arthaud et al., 1975; Ribeiro, 1974). Most of the granitoids of the CIZ are correlated with D_3 and define alignments closely related to the ductile shear zones. These granitoid magmatism, based on emplacement ages (Dias et al., 1998) has been classified as: synorogenic (syn-late and late to post-D_3; 320–300 Ma) and late to post-orogenic (post-D_3; 299–290 Ma).

The granite rock selected for this study is located in the west boundary of the Central Iberian Zone, in northern Portugal. This boundary is marked by one of the most important Variscan structures the Porto-Tomar Shear Zone (Ribeiro et al., 2009). The PTSZ is a north-south subvertical strike-slip fault that is 2 to 8 km wide and extends ca. 170 km from Porto to Tomar (Fig. 1). This important crustal anisotropy controlled the emplacement of the Lavadores granite during the post-collisional stage of the Variscan orogeny. The geology of the studied area is dominated by the presence of metamorphic rocks, intruded by the Lavadores granite. The Lavadores granite outcrops at about 3 km south of Porto in a narrow band along the coastline, in Vila Nova de Gaia, and the massif extended to the south ca. 60 km cutting discordantly Precambrian metamorphic rocks (Chaminé et al., 2003; Oliveira et al., 2010). At southeast, the Lavadores granite has a gradual contact with the Madalena granite (Fig. 1). Most outcrops of the Lavadores granite are, however, covered by sand which difficult fieldwork and sampling. The host rocks, uncharted at this map scale, comprise different lithologies, consisting in gneiss, amphibolites and folded quartz-pelitic metasediments (micaschists and quartz-micaschists). All of these metamorphic rocks present a shearing deformation, related to the last ductile Variscan deformation phase (D_3).

The Lavadores granite has a pinkish colour and presents abundant mafic microgranular enclaves with a wide range of compositions (Silva, 2010; Silva and Neiva, 1998, 2004). This granite is porphyritic, coarse-grained biotite granodiorite-monzogranite and contains quartz + plagioclase (andesine/oligoclase) + perthitic orthoclase and microcline + biotite + zircon + sphene + apatite + allanite ± amphibole. The main petrographic feature that distinguishes this granite is the presence of the accessory phase magnetite, which is uncommon in Late Variscan granites in northern Portugal (Dias et al., 2002; Martins et al., 2009; Mendes and Dias, 2004) and can be considered a magnetite-type granite (Ishihara, 1977). No clear shape preferential orientation of the main minerals was observed in the studied sites. Microstructural observations support the general lack of intracrystaline deformation in minerals, as shown by undeformed biotite and euhedral feldspar crystals, accompanied by large quartz grains. Slight imprints of solid-state deformation are observed, as represented by undulatory extinction in quartz (Fig. 2). Hence, the rock fabric is considered to have developed essentially in the magmatic state.

Available geochemical, mineralogical and isotopic data are reported in several papers (Martins et al., 2003, 2004; Silva, 2010; Silva and Neiva, 1998, 2004).
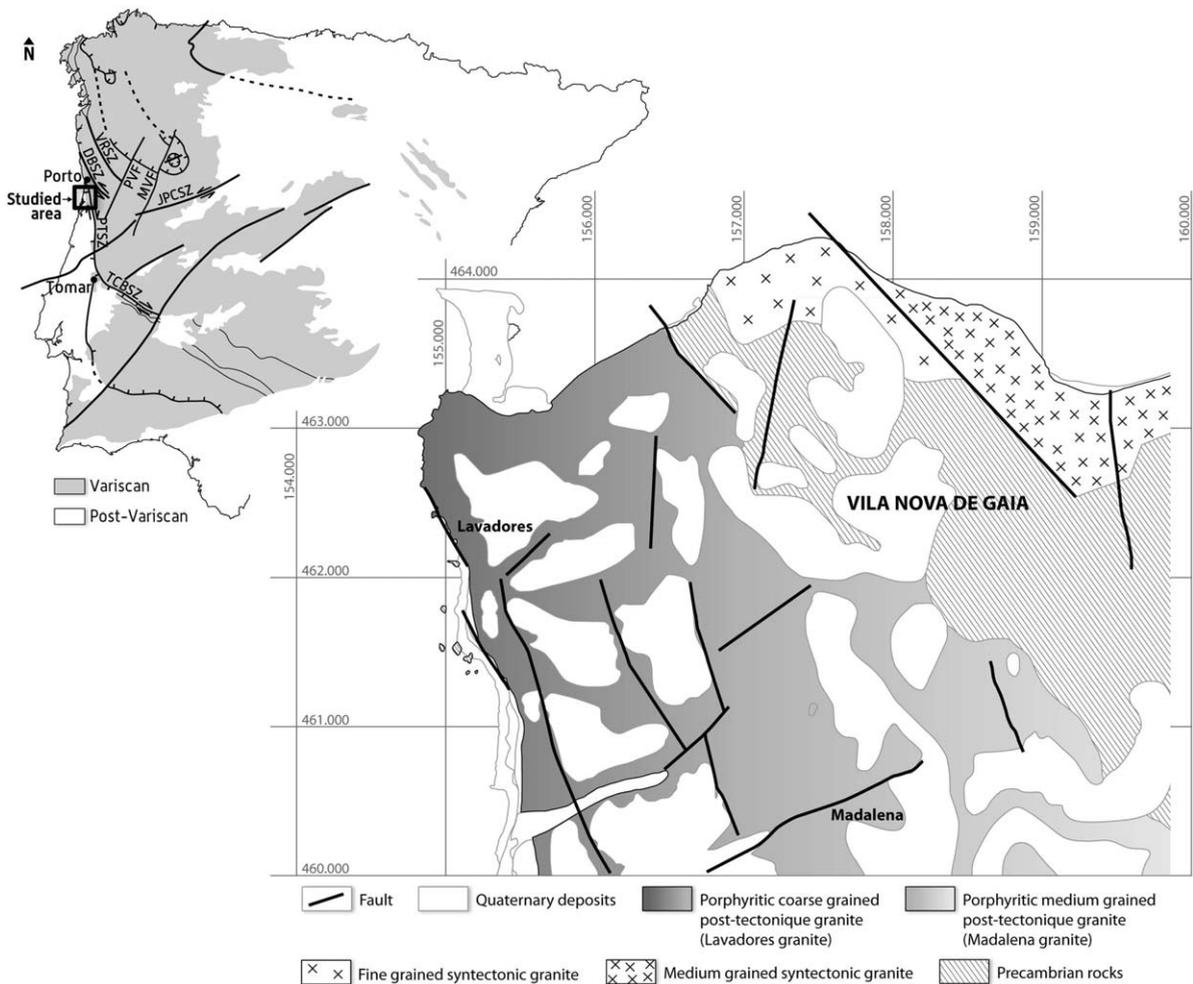
Fig. 1. Geological sketch map of the Lavadores area and its location in northern Portugal (Central Iberian Zone). MVF: Manteigas-Vilariça Fault; PVF: Penacova-Verin Fault; DBSZ: Douro-Beira Shear Zone; JPCSZ: Juzbado-Penalva do Castelo Shear Zone; PTSZ: Porto-Tomar Shear Zone; TCBSZ: Tomar-Cordoba-Badajoz Shear Zone

Fig. 1. Mappe géologique simplifiée de la région de Lavadores et sa localisation au Nord-Ouest du Portugal (Zone Centrale Ibérique). MVF : Faille de Manteigas-Vilariça ; PVF : Faille de Penacova-Verin ; DBSZ : Zone de Cisaillement de Douro-Beira ; JPCSZ : Zone de Cisaillement de Juzbado-Penalva do Castelo ; PTSZ : Zone de Cisaillement de Porto-Tomar ; TCBSZ : Zone de Cisaillement de Tomar-Cordoba-Badajoz.

3. Analytical methods

3.1. Anisotropy of magnetic susceptibility

The AMS studies sampling was performed in the Lavadores granite and also in country-rocks (gneiss, micaschists and amphibolites) (Fig. 4). A total of 3/4 oriented cores were collected at each of the sampling stations corresponding to 63 rock-cylinders, 25 mm in diameter and 22 mm in length, which were prepared for magnetic measurements. Measurements were performed using KLY-4S Kappabridge susceptometer Agico model (Czech Republic) of "Centro de Geologia" of the Porto University. For each site, the AGICO software enabled us to calculate the mean susceptibility Km, which is the mean of the eight (or more) individual arithmetic means $(k1 + k2 + k3)/3$. There also calculated the intensities and orientations of the three axes $K1 \geq K2 \geq K3$, which are the tensorial means of the $k1 \geq k2 \geq k3$ axes for the eight

specimens, and the 95% confidence angles E12, E23 and E31 corresponding to these three axes. The magnetic fabric is defined by the magnetic lineation (parallel to the long axis of the mean ellipsoid orientation average, K1) and the magnetic foliation (plane perpendicular to the orientation of K3, the short axis). P, the magnetic anisotropy ratio, corresponds to K1/K3. To describe the shape of the AMS ellipsoid the shape parameter, T, expressed by

$$T = [2 \ \ln(K2/K3)/\ln(K1/K3)] - 1$$

(Jelinek, 1981) was computed.

A Molspin pulse induction magnetizer was used to create magnetic fields at room temperature to a maximum of 1 T. The magnetization of the representative samples after each exposure was measured with a Molspin spinner magnetometer controlled by a microcomputer. The magnetization obtained in this maximum field was defined as the effective saturation Isothermal Remanent Magnetization value for each of the samples. These
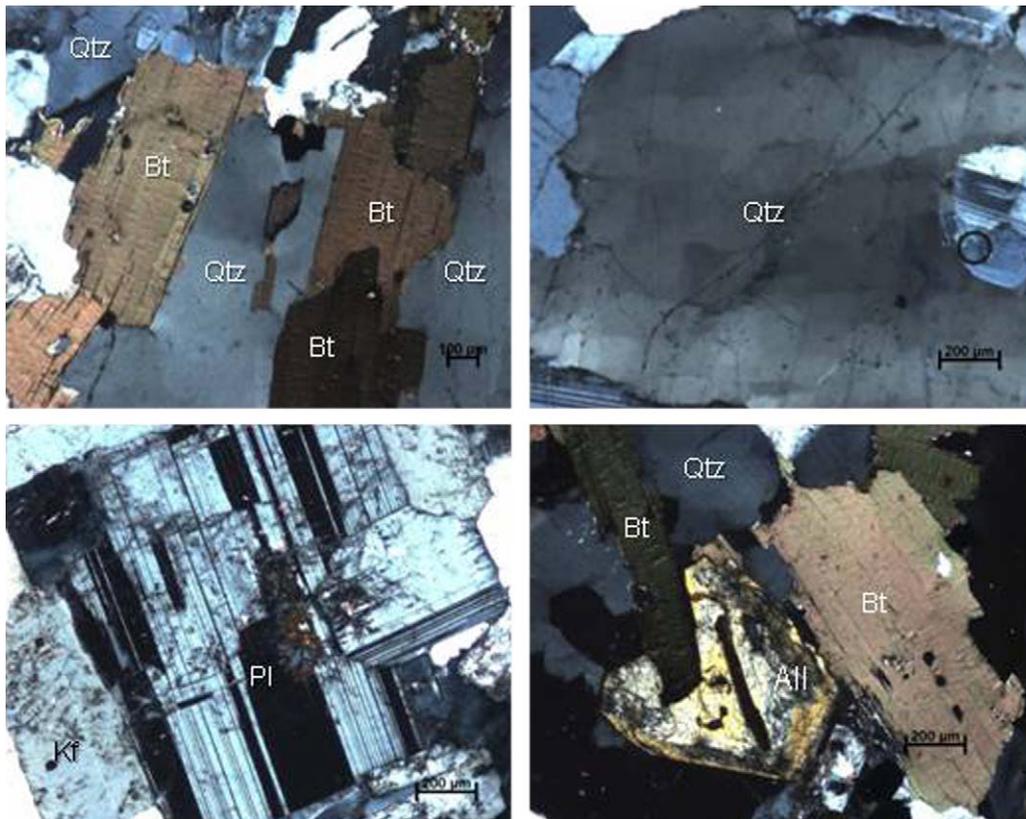
Fig. 2. Magmatic microstructures in the Lavadores granite: undeformed biotite and feldspar and incipient undulatory extinction in quartz. All microphotographs under crossed polars. bt: biotite; Kf: K-feldspar; pl: plagioclase; all: allanite; qtz: quartz.

Fig. 2. Microstructures magmatiques du granite de Lavadores : la biotite et le feldspath ne sont pas déformés, et le quartz présente une légère extinction onduleuse. Toutes les microphotographies ont été prises en lumière polarisée. bt : biotite ; Kf : feldspath potassique ; pl : plagioclase ; all : allanite ; qtz : quartz.

Table 1
Anisotropy of Magnetic Susceptibility data for the sampling sites.

Tableau 1
Résultats des mesures d'anisotropie de susceptibilité magnétique pour les sites d'échantillonnage.

Sampling Sites/ Lithology	Km E^{-6} SI	P	T	K1		K3		Foliation	E12	E23	E31	n
				Dec	Inc	Dec	Inc					
LV1– Lavadores granite	16477.50	1.116	0.292	245	69	31	18	N121; 72SW	37	11	8	12
LV2– Lavadores granite	17426.67	1.206	–0.246	194	81	23	4	N144; 83 SW	*	*	*	3
LV3– Lavadores granite	17031.43	1.164	–0.106	200	72	12	18	N102; 72 SW	29	10	9	7
LV4– Lavadores granite	10589.00	1.144	0.214	241	79	20	9	N119; 81 SW	8	16	5	9
LV5– Lavadores granite	19302.86	1.192	–0.028	171	78	355	12	N085; 78 S	12	6	7	7
LV6– Lavadores granite	15000.00	1.251	–0.285	248	80	21	8	N111; 82 SW	*	*	*	2
Amphibolite	1348.88	1.311	–0.253	226	62	340	12	N070; 78 SE	5	20	4	7
Micaschist	3965.56	1.932	–0.060	219	58	52	31	N142; 59 SW	18	28	8	9
Gneiss	22.71	1.034	0.079	316	77	123	23	N33; 77 NE	49	73	57	7

Km: mean susceptibility in 10^{-6} SI; P: anisotropy degree; T: shape parameter (Jelinek, 1981); Dec, Inc: declination, inclination; E12, E23 and E31: 95% confidence angles corresponding to the three axes; n: number of specimens. *: not enough data for statistics.
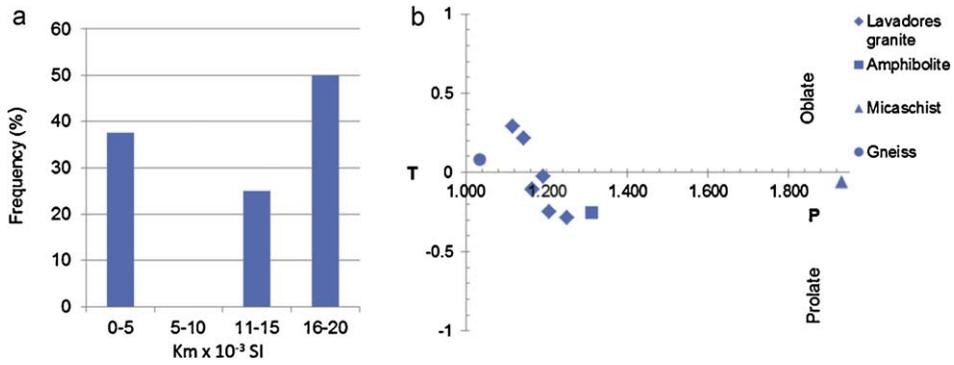
Fig. 3. a: frequency histogram for bulk magnetic susceptibility; b: plots of the shape (T) and anisotropy (P) parameters showing dominant prolate ellipsoids.

Fig. 3. a : histogramme de fréquence pour la susceptibilité magnétique ; b : représentation du paramètre de forme (T) et du paramètre d'anisotropie (P) montrant des ellipsoïdes allongés.
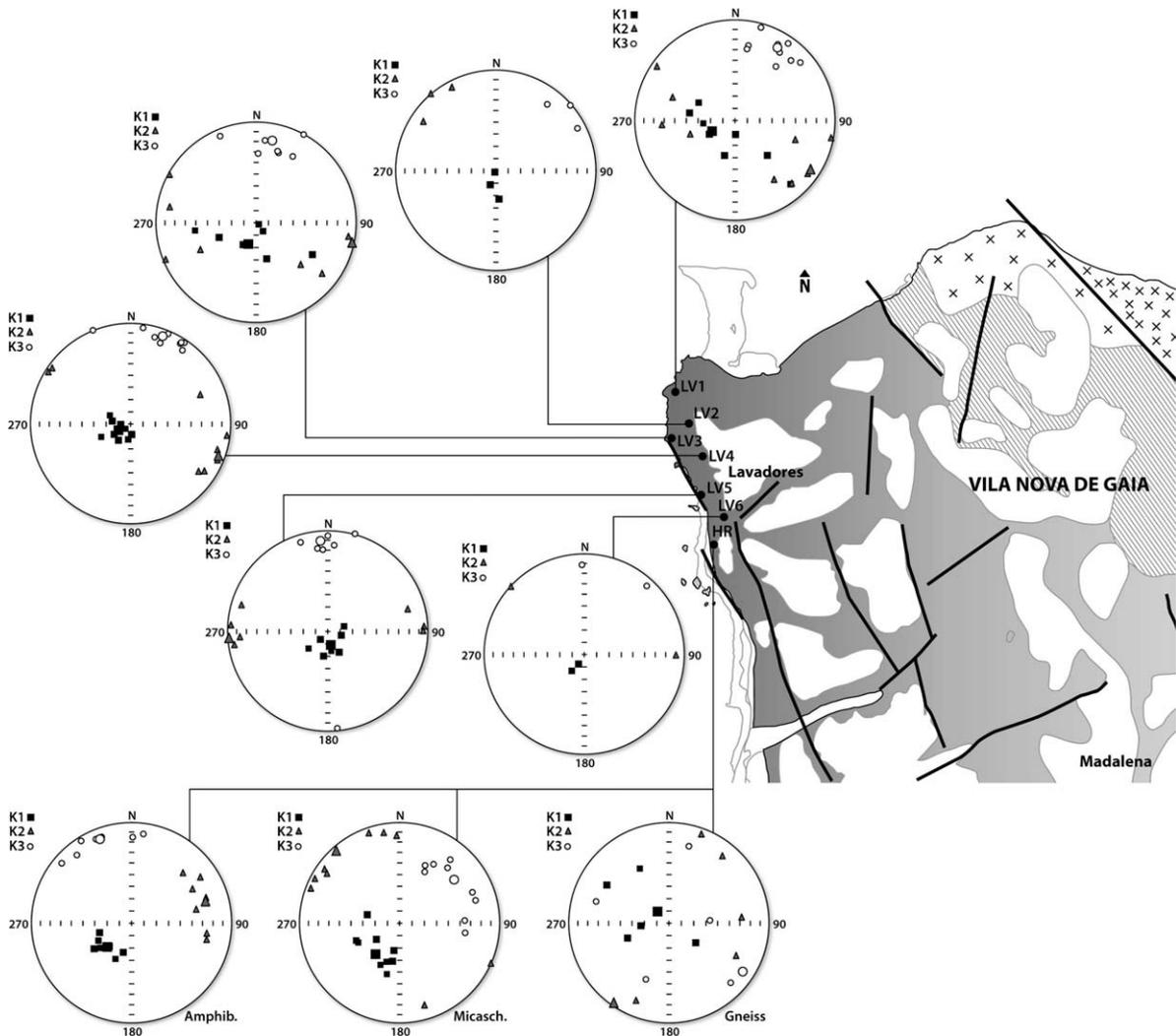
Fig. 4. Simplified geological map of the studied area with the sampling sites and the stereograms (Schmidt, lower hemisphere) of the magnetic fabrics.

Fig. 4. Carte géologique simplifiée de la zone étudiée avec les sites d'échantillonnage et les stéréogrammes (Schmidt, hémisphère inférieur) de fabrique magnétique.

measurements were performed in the Earth Sciences Department of the University of Coimbra.

3.2. U–Pb dating

The U–Pb isotopic analyses were carried out at CRPG, Nancy, France, using a conventional U–Pb method on multigrain zircon fractions. The zircons were recovered by crushing the sample and sieving, followed by heavy liquid and magnetic separations and finally hand picking. Four zircon fractions were selected according to their morphology, colour, and lack of inclusions, fractures and metamictisation.

Some of these fractions were submitted to air-abrasion (Krogh, 1982) to eliminate the external zones of the crystal where Pb loss may have occurred. All zircon fractions were observed on a backscattered scanning electron microscopy (BSEM). Chemical preparation of U and Pb analysis includes:

- HNO_3 3 N warm washing of the zircon;
- HF digestion at 240 °C and HCl 3 N dissolution of the fluorides at 180 °C in a Teflon bomb (Parrish, 1987);
- separation of Pb and U by elution on anionic resin of two aliquots (one with the addition of a mixed ^{208}Pb-^{235}U spike) following Krogh (1973).

Common Pb blanks varied from 30 and 80 pg during this study.

4. Results

4.1. Anisotropy of Magnetic Susceptibility (AMS)

The results for the nine stations are summarized in Table 1.

The magnetic susceptibility values fall into two major groups: $K > 10 \times 10^{-3}$ SI for the Lavadores granite and $K < 5 \times 10^{-3}$ SI for the amphibolite, metasediments and gneiss as is shown on the K histogram (Table 1 and Fig. 3a).

The magnetic anisotropy, P, has values always higher than 1.10 in the amphibolite, metasediments and Lavadores granite and less than 1.10 in the gneiss.

The shape parameter T is below zero in six sites, which is indicative of prolate AMS ellipsoids: in metasediments, amphibolite and four sites of the Lavadores granite. The gneiss and two sites of the Lavadores granite show oblate ellipsoids (Table 1).

The plot of the T and P parameters show that the prolate shape of the AMS ellipsoid is related to the highest anisotropies (Fig. 3b).
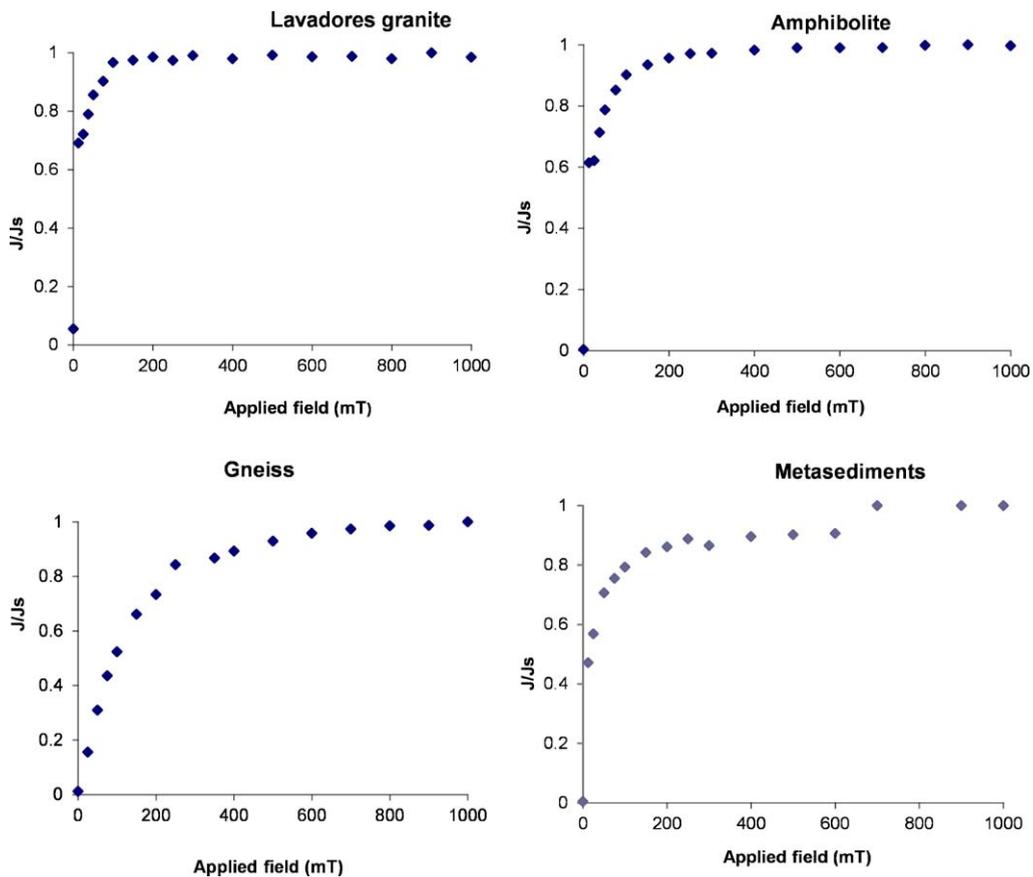
Fig. 5. Isothermal Remanent Magnetization (IRM) acquisition curves for representative samples. Js: saturation magnetization; J: magnetization.

Fig. 5. Courbes d'acquisition d'aimantation rémanente isotherme pour les échantillons représentatifs. Js : aimantation à saturation ; J : aimantation.

Table 2

U–Pb isotopic data on zircon from the Lavadores granite, northern Portugal. The atomic ratios were corrected for initial common lead composition blanks (Stacey and Kramers, 1975) and mass fractionation using NBS 983 Standard. The U–Pb ages with 2σ errors were calculated using a version of Isoplot program (Ludwig, 2003). The decay constants used for age determinations are from Steiger and Jäger (1977).

Tableau 2

Résultats analytiques U–Pb des zircons provenant du granite de Lavadores, Nord-Portugal. Les rapports isotopiques ont été corrigés des blancs, de la composition du plomb commun initial (Stacey et Kramer, 1975) et du fractionnement de masse (NBS 983 Standard). Les âges U–Pb, les erreurs 2σ, ont été calculés à l'aide d'une version du programme Isoplot (Ludwig, 2003). Les constantes de désintégration, utilisées pour les déterminations d'âge sont de Steiger et Jäger (1977).

Fractions (shape)	Weight (mg)	Concentrations			Isotopic ratios			Apparent ages (Ma)		
		U Total (ppm)	Pb* (ppm)	$^{206}Pb/^{204}Pb$	$^{206}Pb^*/^{238}U$ 2σ(%)	$^{207}Pb^*/^{235}U$ 2σ(%)	$^{207}Pb^*/^{206}Pb^*$ 2σ	$^{206}Pb^*/^{238}U$ 2σs	$^{207}Pb^*/^{235}U$ 2σ	$^{207}Pb^*/^{206}Pb^*$ 2σ
Lav99 (Z)[b] (needle)	0.95	1486.7	63.1	1763.79	0.04222 ± 0.084522	0.304251 ± 0.239064	0.052265 ± 0.158541	266.6 ± 0.2	269.7 ± 0.6	297 ± 4
Lav99 (Z)[b] (short prisms)	21	1665.9	69.1	1313.71	0.041804 ± 0.182463	0.301108 ± 0.369571	0.05224 ± 0.191685	264 ± 0.5	267.3 ± 0.9	296 ± 4
Lav99 (Z)[b] (flat)	0.16	1183.9	48.7	1032.34	0.040716 ± 0.212583	0.293165 ± 0.410623	0.05222 ± 0.2056772	257.3 ± 0.5	261 ± 0.9	295 ± 5
Lav99 (Z)[a] (long prisms)	0.43	1343.9	58	1628.11	0.04306 ± 0.120448	0.310184 ± 0.2559	0.052245 ± 0.13844	271.8 ± 0.3	274.3 ± 0.6	296 ± 3

Pb* : radiogenic lead.
[a] Fraction submitted to abrasion.
[b] Fraction not submitted to abrasion.

Equal-area stereographic projections of the three principal axes of magnetic susceptibility each site are presented in Fig. 4.

The Lavadores granite has very homogeneous magnetic lineations with steep dip (mean dip is 79°) trending to N203°. The magnetic foliations have also steep dip (mean dip is 77° SW) and trend to N113°.

In amphibolites and metasediments, the magnetic lineations are also subvertical. Nevertheless, in the gneiss, the magnetic lineations are poorly defined. The magnetic foliation of the metasediments have WNW-ESE trend and dip to south-west (similar to Lavadores granite). In the amphibolites, the magnetic foliation has a NE-SW trend and is subvertical.

Finally the foliation in the gneiss is subvertical with WNW-ESE trend; however, the low magnetic anisotropy of this facies, creates a wide dispersion of the AMS axes which implies a bad definition of the magnetic foliation and lineation.

The Isothermal Remanent Magnetization data obtained point out three distinct magnetic behaviors: in the granite the IRM data are due to the ferrimagnetic fraction; in the metasediments and amphibolites are due to both the paramagnetic and ferrimagnetic fractions; finally the gneiss values are controlled by the paramagnetic fraction (Fig. 5).

4.2. U–Pb geochronology

The analytical data and calculated ages with 2σ errors from Lavadores granite are presented in Table 2. The U–Pb zircon data were carried out on four zircon fractions of one sample of the Lavadores granite. A typological study (Pupin, 1980) has allowed the identification of several zircon types (Martins et al., 2003, 2004). The zircons are very limpid, colourless or light rose color. The back-scattered scanning electron microscope imaging of the long prismatic zircons revealed an inner zone, sometimes partially resorbed, surrounded by a finely magmatic zoned rims. Some of them have cores that could correspond to an earlier magmatic crystallization. The prismatic acicular
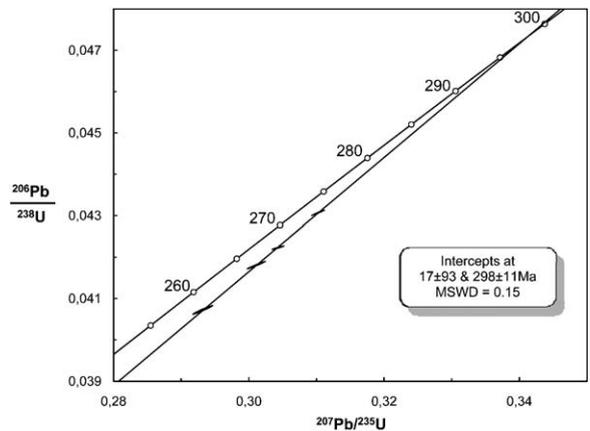
Fig. 6. U-Pb Concordia diagram showing analytical data for zircon fractions from the Lavadores granite, northern Portugal.

Fig. 6. Diagramme Concordia du granite de Lavadores, Nord-Portugal.

and flat zircons are more homogeneous crystals devoid of cores and showing generally a faint zoning.

The four zircon fractions are concordant and define a line (MSWD of concordance = 0.013, probability of fit = 0.99) intersecting the Concordia at 298 ± 11 Ma (Fig. 6) that can be interpreted as the emplacement age of this granite. This new data do not confirm the age of 314 ± 11 Ma obtained by Silva (1995) using the Rb/Sr method, although the error bars are large for the two of them, since the Lavadores granite shows no evidence of being syntectonic. In fact the new age and thus the post-tectonic character is in agreement with geological and tectonic settings and corresponds to the age of Variscan late-orogenic granite magmatism, post-D$_3$ (Dias et al., 1998, 2009; Ferreira et al., 1987; Martins et al., 2009).

5. Discussion and conclusion

Granite bodies record the tectonic events that are related to their emplacement during magma cooling, through the orientation of the magmatic foliation and lineation, and trough solid-state deformation at high and low temperature that record the kinematics of deformation as crystallization progress (Be Mezeme et al., 2007; Gleizes et al., 2006; Verner et al., 2009). Based on petrographic overview and AMS data, we argued that the Lavadores granite structure indicates fabrics developed at a magmatic stage during magma crystallization.

Based on the AMS measurements, the inclusion of the magnetic susceptibility values in two large groups ($K > 10^{-3}$ SI and $K < 10^{-4}$ SI) allows the characterization of the magnetic behaviour of the studied facies. According to Tarling and Hrouda (1993), in a rock presenting $K > 10^{-3}$ SI, its susceptibility and anisotropy are due to the ferrimagnetic fraction (magnetite); if $K < 10^{-4}$ SI then the paramagnetic fraction controls the magnetic susceptibility and anisotropy of the rock.

Isothermal Remanent Magnetization (IRM) data pointed out two distinct magnetic behaviours: in the granites and metasediments, the IRM data are due to a ferrimagnetic fraction and in the gneiss values are controlled by the paramagnetic one (Sant'Ovaia et al., 2009).

In the case of Lavadores granite, the presence of magnetite can include this granite in the series of "magnetite type granites" defined by (Ishihara, 1977). In the case of the gneiss, the magnetic susceptibility is mainly due to iron-bearing minerals such as the biotite.

The Lavadores granite shows a high magnetic anisotropy (the average for the six sampling stations is 1.179). Even so, field and microscope observations do not show signs of low temperature solid-state deformation. Occasionally some magmatic flow is visible on the field and magmatic to high temperature solid-state deformation microstructures are present. Apparently this anisotropy is due solely to the fact that the bearer of the magnetic signal is the magnetite (which has a high susceptibility) and, though a weak alignment of magnetite grains leads to a higher anisotropy to the rock. The "subfabric" of magnetite prevails over any other "fabric" mineral, especially that of biotite or amphibole. In addition, the "subfabric" of magnetite is reflected generally in the constrict shape of AMS ellipsoids.

The magnetic foliations presents generally high dips and most of the magnetic lineations are subvertical; it is also worth noting that prolate ellipsoids characterize the studied granite. These features might suggest the presence of a feeding zone for the Lavadores granite. In this zone, the magma ascended into a conduit, the PTSZ anisotropy, towards upper-crustal levels. The Lavadores granite emplacement was controlled by transtensional structures associated with the PTSZ, which create offsets for magma emplacement, as attested by the magnetic subvertical WNW-ESE foliation associated with subvertical magnetic lineations. This magnetic fabric pattern probably records the evolution of regional tectonics during or just after the complete crystallization of the magma because only magmatic microstructures are present rather than low temperature solid-state microstructures.

In the metasediments and gneiss, the NW-SE magnetic foliations are concordant with the foliation measured in the field. In the case of metasediments the magnetic anisotropy (mean 1.932) may not be justified exclusively by the presence of magnetite. A deformation event must be taking into account as well, to explain the high magnetic anisotropy. However in the gneisses the magnetic anisotropy (mean 1.034) is an indicator of an incipient foliation and is similar with the values found in syntectonic peraluminous granites of the Central Iberian Zone (Sant'Ovaia and Noronha, 2005).

The subvertical lineations found in the metasediments are parallel to the subvertical folds axes, which are observed in the field.

The Rb-Sr age (314 ± 11 Ma) previously obtained in the Lavadores granite cannot represent an emplacement age since structural studies have evidenced a late tectonic emplacement (Late Carboniferous-Permian) of the granite body rather than a syntectonic emplacement. The lack of internal structures led to a model of magma ascent and emplacement after the last Variscan folding event occurred. In addition, the country rocks are clearly deformed by this Variscan event, which predates pluton emplacement.

The U-Pb zircon age 298 ± 11 Ma obtained in the present study is consistent with field relationships and structural data and suggest a post-tectonic emplacement. This post-tectonic feature of the Lavadores granite is also supported by the magmatic nature of the microstructures, which suggest that the magma did not suffer further significant deformation once crystallized.

In spite of a limited number of data, we may propose that the Lavadores granite can be considered a late to post-orogenic (post-D$_3$-290-299) granite with an age constrained to 298 ± 11 Ma whose emplacement was controlled by the WNW-ESE local structures linked with a dextral movement in this sector of the north-south trending PTSZ. Nevertheless, tectonic control was only moderated since no related low temperature solid-state microstructures appear.

France) and to the CEMUP (Porto University) for SEM analyses. We would like to thank to an anonymous reviewer and to Aude Gébelin for constructive comments that helped to greatly improve the manuscript.

References

Arthaud, F., Matte, Ph, 1975. Les décrochements tardi-hercyniens du Sud-Ouest de l'Europe. Géométrie et essai de reconstituition des conditions de la déformation. Tectonophysics 25 (1/2), 139–171.

Be Mezeme, E., Faure, M., Chen, Y., Cocherie, A., Talbot, J.-Y., 2007. Structural AMS and geochronological study of a laccolith emplaced during Late Variscan orogenic extension: the Rocles pluton (SE French Massif Central). Int. J. Earth Sci. 96, 215–228.

Castro, A., 1986. Structural pattern and ascent model in the central Extremadura Batholit, Hercynian Belt, Spain. J. Struct. Geol. 8, 633–645.

Chaminé, H., Gama Pereira, l., Fonseca, P.E., Noronha, F., Lemos de Sousa, M.J., 2003. Tectonostratigraphy of the Porto-Albergaria-a-Velha-Coimbra-Tomar shear zone between Central-Iberian and Ossa-Morena Zones (Iberian Massif, W Portugal). Cad. Lab. Xeolóxico de Laxe 28, 37–78.

Dias, R., Ribeiro, A., 1995. The Ibero-Armorican Arc: a collision effect against an irregular continent? Tectonophysics 246, 113–128.

Dias, G., Leterrier, J., Mendes, A., Simões, P., Bertrand, J.M., 1998. U-Pb zircon and monazite geochronology of syn- to post-tectonic Hercynian granitoids from the central Iberian Zone (northern Portugal). Lithos 45, 349–369.

Dias, G., Noronha, F., Simões, P.P., Almeida, A., Martins, H.C.B., Ferreira, N., 2009. Geochronology and petrogenesis of Late-Variscan plutonism (NW Portugal): Synthesis and inferences on crustal recycling and growth. Geochim. Cosmochim. Acta. 73 (13), A288 Special supplement.

Dias, G., Simões, P.P., Ferreira, N., Leterrier, J., 2002. Mantle and crustal sources in the genesis of late-Hercynian granitoids (NW Portugal): geochemical and Sr-Nd isotopic constraints. Gondwana Research 5 (2), 287–305.

Faure, M., 1995. Late Carboniferous extension in the Variscan French Massif Central. Tectonics 14, 132–153.

Faure, M., Pons, J., 1991. Crustal thinning recorded by shape of the Namurian-Wesphalian leucogranite in the Variscan Belt of the Northwest Massif Central, France. Geology 19, 730–733.

Faure, M., Monie, P., Pin, C., Malusky, H., Leloix, C., 2002. Late Visean thermal event in the northern part of the French Massif Central: new $^{40}Ar/^{39}Ar$ and Rb-Sr isotopic constraints on the Hercynian syn-orogenic extension. Int. J. Earth Sci. 91, 53–75.

Fernández-Suárez, J., Gutierrez-Alonso, G., Johnston, S.T., Jeffries, T.E., Pastor-Gálan, D., 2011. Iberian late-Variscan granitoids: some considerations on crustal sources and the significance of "mantle extraction ages". Lithos 123 (1-4), 121–132.

Ferreira, N., Iglésias, M., Noronha, F., Pereira, E., Ribeiro, A., Ribeiro, M.L., 1987. Granitos da Zona Centro Ibérica e seu enquadramento geodinâmico. In: Bea, F., Carnicero, A., Gonzalo, J., Lopez Plaza, M., Rodriguez Alonso, M. (Eds.), Geología de los Granitoides y Rocas Asociadas del Macizo Hesperico. Editorial Rueda, Madrid, pp. 37–51. Libro de Homenaje a L.C. García de Figuerola.

Gébelin, A., Brunel, M., Monie, P., Faure, M., Arnaud, N., 2007. Relationships between Carboniferous magmatism and ductile shear zones in the Limousin (Massif Central, France). Tectonics 26 (TC2008), 2007, doi:10.1029/2005CT001822.

Gébelin, A., Martelet, Chen, Y., Brunel, M., Faure, M., 2006. Structure of Late Variscan Millevaches leucogranite massif in the French Massif Central: AMS and gravity modelling results. J. Struct. Geol. 28 (1), 148–169.

Gébelin, A., Roger, F., Brunel, M., 2009. Syntectonic crustal melting and high-grade metamorphism in a transpressional regime, Massif Central, France. Tectonophysics 477 (3–4), 229–243.

Gleizes, G., Crevon, G., asrat, A., Barbey, P., 2006. Structure, age and mode of emplacement of the Hercynian Boedères-Louron pluton (Central Pyrenees, France). Int. J. Earth Sci. 95, 1039–1052.

Hutton, D.H.W., 1988. Granite emplacement mechanisms and tectonic controls: inferences from deformation studies. Trans. R. Soc. Edinburg: Earth Sciences 79, 245–255.

Ingram, G.M., Hutton, D.H.W., 1994. The Great Tonalite Sill: Emplacement into a contractional shear zone and implications for Late Cretaceous to Early Eocene tectonics in southeastern Alaska and British Columbia. Geol. Soc. Am. Bull. 106, 715–728.

Ishihara, S., 1977. The Magnetite-series and Ilmenite-series Granitic Rocks. Mining Geology 27, 292–305.

Jelinek, V., 1981. Characterization of the magnetic fabric of rocks. Tectonophysics 79, 63–67.

Joly, A., Faure, M., Martelet, G., Chen, Y., 2009. Gravity inversion, AMS and geochronological investigations of syntectonic granitic plutons in the southern part of the Variscan French Massif Central. J. Struct. Geol. 3, 421–443.

Krogh, T.E., 1973. A low-contamination method for hydrothermal decomposition of zircon and extraction of U and Pb for isotopic age determination. Geochim. Cosmochim. Acta. 48, 505–511.

Krogh, T.E., 1982. Improved accuracy of U-Pb zircon ages by the creation of more concordant systems using an air abrasion technique. Geochim. Cosmochim. Acta. 46, 637–649.

Lagarde, J.L., Capdevila, R., Fourcade, S., 1992. Granites et collision continentale: l'exemple des granitoïdes carbonifères dans la chaîne hercynienne ouest-européenne. Bull. Soc. geol. France 163 (5), 597–610.

Ludwig, K.R., 2003. Isoplot 3. 00: A Geochronological Toolkit for Microsoft Excel. Berkeley Geochronology Center, Special Publication nº 4, 74p.

Martins, H.C.B., Sant'Ovaia, H., Eusébio, N., Noronha, F., 2003. Zircon typology and magnetic susceptibility of late Variscan biotite granites in Porto area (northern Portugal). Memórias e Notícias 2, 7–17.

Martins, H.C.B., Sant'Ovaia, H., Eusébio, N., Noronha, F., 2004. Magnetic susceptibility and zircon typology of a magnetite and ilmenite-type granites of (Northern Portugal). Geochim. Cosmochim. Acta. 68 (11), A658 Special supplement,.

Martins, H.C.B., Sant'Ovaia, H., Noronha, F., 2009. Genesis and emplacement of felsic Variscan plutons within a deep crustal lineation, the Penacova-Régua-Verín fault: an integrated geophysics and geochemical study (NW Iberian Peninsula). Lithos 111, 142–155.

Matte, P., 1991. Accretionary history and crustal evolution of the Variscan Belt in Western Europe. Tectonophysics 196, 309–337.

Mendes, F., 1967. Contribution à l'étude géochronologique, par le méthode au strontium, des formations cristallines du Portugal. Bol. Mus. Lab. Min. Geol., Univ. Lisboa. 11 (1), 155p.

Mendes, A.C., Dias, G., 2004. Mantle-like Sr-Nd isotope composition of Fe-K subalkaline granites: the Peneda-Gerês Variscan massif (NW Iberian Peninsula). Terra Nova 16, 109–115.

Noronha, F., Ramos, J.M.F., Rebelo, J.A., Ribeiro, A., Ribeiro, M.L., 1979. Essai de corrélation des phases de déformation hercynienne dans le Nord-Ouest péninsulaire. Boletim da Sociedade Geológica de Portugal 21, 227–237.

Oliveira, M., Noronha, F., Lima, A., 2010. Geological mapping at a scale of 1:10 000 of the SW area of the 9C Geological sheet. Porto. e-Terra 22 (16), 1–4.

Parrish, R.R., 1987. An improved micro-capsule for zircon dissolution in U-Pb geochronology. Chem. Geol. 66, 99–102.

Pereira, M.F., Silva, J.B., Drost, K., Chichorro, M., Apraiz, A., 2010. Relative timing of transcurrent dispacements in northern Gondwana: U-Pb laser abation ICP-MS zircon and monazite geochronology of gneisses and sheared granites from the western Iberian Massif (Portugal). Gondwana Research 17, 461–481.

Pupin, J.P., 1980. Zircon and granite petrology. Contr. Mineral. Petrol. 110, 463–472.

Ribeiro, A., 1974. Contribution à l'étude tectonique de Trás-os-Montes Oriental. Comunicações dos Serviços Geológicos de Portugal 24, 1–168.

Ribeiro, A., Munhá, J., Mateus, A., Fonseca, P., Pereira, E., Noronha, F., Romão, J., Rodrigues, J., Castro, P., Meireles, C., Ferreira, N., 2009. Mechanics of thick-skinned Variscan overprinting of Cadomian basement (Iberian Variscides). C. R. Geoscience 341, 127–139.

Ribeiro, A., Pereira, E., Dias, R., 1990. Structure in the Iberian Península. In: Dallmeyer, R.D., Martinez, G. (Eds.), Pre-Mesozoic Geology of Iberia. Springer-Verlag, Berlin, pp. 220–236.

Sant'Ovaia, H., Noronha, F., 2005. Gravimetric anomaly modelling of the post-tectonic granite pluton of Águas Frias–Chaves (northern Portugal). Cad. Lab. Xeol. Laxe. Coruña 30, 75–86.

Sant'Ovaia, H., Ribeiro, M.A., Gomes, C., 2009. Magnetite-bearing mineral assemblages in igneous and metamorphic facies (North Portugal). Geochim. Cosmochim. Acta. 73 (13), A1115 Special supplement.

Silva, M.M.V.G., 1995. Mineralogia, petrologia, e geoquímica de encraves de rochas graníticas de algumas regiões Portuguesas. PhD thesis, Coimbra University. Portugal, 288p, unpublished.

Silva, M.M.V.G., 2010. The Lavadores granite and its enclaves. In: Cotelo Neiva, J.M., Ribeiro, A., Mendes V., Noronha, F., Magalhães Ramalho, (Eds.), Ciências Geológicas–Ensino e Investigação e sua História, vol 1, pp. 269–279.

Silva, M.M.V., Neiva, A.M., 1998. Geoquímica de encraves microgranulares e granitos hospedeiros da região de Vila Nova de Gaia, Norte de Portugal, Actas do V Congresso Nacional de Geologia. Comunicações r203õesdoInstitutoGeológicoeMineiro, Lisboa84(1), B − 35 − B − 38.

Silva, M.M.V., Neiva, A.M., 2004. Geochemistry of high-Mg-K microgranular enclaves and host granites from Vila Nova de Gaia, northern Potugal. Geochim. Cosmochim. Acta. 68 (11), A658.

Speer, J.A., Sween, H.Y., Gates, A.E., 1994. Generation, segregation, ascent and emplacement of Alleghanian plutons in the Southern Appalachians. J. Geology. 102, 249–267.

Stacey, J.S., Kramers, J.D., 1975. Approximation of terrestrial lead isotope evolution by a two-stage model. Earth Planet. Sci. Lett. 26, 207–221.

Steiger, R.H., Jäger, E., 1977. Subcomission on Geochronology: convention in the use of decay constants in geo- and cosmochronology. Earth Planet. Sci. Lett. 36, 359–362.

Tarling, D.H., Hrouda, F., 1993. The magnetic anisotropy of rocks. Chapman & Hall, London, 217p.

Tikoff, B., Saint Blanquat, M., 1997. Transpressional shearring and strike-slip partitioning in the Late Cretaceous Sierra Nevada magmatic arc, California. Tectonics 16, 442–459.

Verner, K., Žák, J., Petroldová, J., Šramek, J., Sedlák, J., Trubač, J., Týcová, P., 2009. Magmatic history and geophysical signature of a post-collisional intrusive center emplaced near a crustal-scale shear zone: the Plechý pluton (Moldanubian batholit Bohemian Massif). Int. J. Earth Sci. (Geol. Runsch.) 98 (3), 517–532.